



Cite this: *Chem. Commun.*, 2014, 50, 13296

Received 29th June 2014,
Accepted 27th August 2014

DOI: 10.1039/c4cc04817b

www.rsc.org/chemcomm

A cellulose based hydrophilic, oleophobic hydrated filter for water/oil separation†

Kathleen Rohrbach,‡ Yuanyuan Li,‡ Hongli Zhu, Zhen Liu, Jiaqi Dai, Julia Andreasen and Liangbing Hu*

A hydrated regular cellulose paper filter modified with nanofibrillated cellulose (NFC) hydrogel was successfully fabricated for water/oil separation. The fabricated filter's hydrophilic and oleophobic properties resulted in increased filter life and decreased environmental impact, while displaying water flux of $89.6 \text{ L h}^{-1} \text{ m}^{-2}$ with efficiency $\geq 99\%$ under gravitational force.

Today's energy industry relies largely on petroleum-based oil. Separating water/oil emulsions is of worldwide urgency due to frequent oil spills and increasing oil pollution from industrial wastewater. Trace amounts of water can be found in crude oil which needs to be separated out before use.¹ However, energy-efficient and cost-effective separation of water from oil is a great challenge due to the high stability and viscosity of water/oil emulsions.² It has been considered that surfactants on the water/oil interface create stable water/oil emulsions, due to surfactants aggregation and formation of networks around the molecules.³ A number of technologies have been developed for water/oil separation, including pressurized membrane based separation, treatment with chemical demulsifiers, chemical-free demulsification methods with microwave, electrical field, and heating.^{2,4–9}

Membrane based demulsification methods are attractive because: (1) they show a higher energy efficiency than some of the other methods stated above; and (2) there are a range of materials that can be designed to selectively filter either water or oil. In the past ten years, a range of materials have been demonstrated to filter or adsorb oil from water, referred to as "oil-removing" materials. These materials include polydimethylsiloxane (PDMS) coated nanowire membranes, polytetrafluoroethylene (PTFE) coated metal mesh, carbon based porous materials, crosslinked polymer gels, *etc.*^{8–12} However, oil-removing materials are easily fouled and clogged by oil because of their oleophilic properties.¹³ In most cases, the adhered

oil is hard to be removed and easily causes secondary pollution when discarded. Many of these filters run off of pumps, consuming even more energy and decreasing efficiency.² Secondary pollution, oil fouling, and increased energy needs have a detrimental impact to the environment. These factors are moving interests away from using "oil-removing" materials toward hydrophilic/oleophobic filters in water/oil separations.¹² However, existing hydrophilic/oleophobic filter technologies are modified using harmful chemicals such as fluoride groups to create the filter's oleophobic behaviour,^{13–18} so improvements still need to be made to decrease their environmental impact.

The nanocellulose-based filter created in this study is capable of improving current technology by increasing efficiency and reducing clogging with environmentally friendly, renewable cellulose material. The inherent challenge in creating a hydrophilic/oleophobic filter is that water has a higher surface energy than oil. Therefore, any filter which has a lower surface energy than oil, causing repulsion of the oil based on Young's equation, will also exhibit hydrophobic behaviour.^{11,13} As shown in Fig. 1, coating the filter with a layer of nanofibrillated cellulose (NFC) hydrogel, through a dipping and drying process, takes advantage of hydrogel's hydrophilic behaviour.¹⁷ This behaviour causes the filter to absorb water until reaching saturation when it creates a hydration layer.¹³

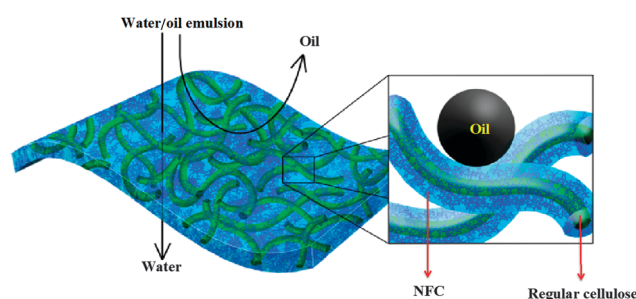


Fig. 1 Schematic of water oil separation using a hydrated filter. Water passes through, while oil is retained above. The filter is a regular cellulose paper with a layer of coated cellulose hydrogel. The oil droplets repulsion is due to the surface energy between the hydrogel and oil, the oil–water–hydrogel interface, and the roughness of the hydrogel surface.

Department of Materials Science and Engineering, University of Maryland College Park, MD 20742, USA. E-mail: binghu@umd.edu

† Electronic supplementary information (ESI) available. See DOI: 10.1039/c4cc04817b

‡ These authors contributed equally to this work.

The triple interface layers of hydrogel, water, and oil enhance the oleophobic behaviour.¹⁴ The roughness of the hydrogel traps water in the microscopic crevices.¹¹ The big difference in surface energy between oil and water keeps oil from penetrating the filter. Without the coating, both oil and water are capable of penetrating through the filter. Hydrating this coating generates oleophobic behaviour, while retaining hydrophilicity without using traditional functionalization groups (Fig. S1, ESI[†]). The hydrophilic/oleophobic behaviour is uniquely created by taking advantage of the different properties and structures of cellulose at both the macroscopic and nanoscopic scale without introducing any harmful chemicals.

The NFC used in this paper is about 10 nm to 40 nm in diameter shown in Fig. 2a. NFC was fabricated similar to the literature.¹⁹ The NFC was modified with citric acid to promote crosslinking of the hydrogel, using a method similar to that reported by C. Demitri *et al.*²⁰ A NFC–citric acid mixture was made with a weight ratio of 0.0030 citric acid : 1 NFC. Wood pulp filters with a average pore size of 150 μm were then dipped into the NFC solution and left to dry at 25 $^{\circ}\text{C}$ for 24 hours. After drying, the filters were placed in an oven at 80 $^{\circ}\text{C}$ to initiate the crosslinking reaction, which occurred due to esterification of carboxylic acids groups with cellulosic hydroxyl groups.²⁰ Crosslinking the hydrogel adds stability and strength to the coating, preventing removal or breakdown of the coating during the filtration process and increasing the filters' lifetime. The filtration process was purely driven by gravity instead of by the traditionally used pumps. This change reduces the energy needed during the water/oil separation processes, making the process more efficient and reducing the impact of the process on the environment. The majority of other current hydrophilic/oleophobic filter technology requires functionalization through nanomaterial coatings that cover prepared metal meshes with microscopic pores and/or polymerization,^{13–17,21–25} which requires high manufacturing cost. This filter's production cost is small and the process is scalable, since manufacturing only requires a dipping and drying process and the raw materials

needed are inexpensive. When considering production and implementation of new water/oil separation filters, industrial needs in oil refinement and wastewater treatment searches for cost effective, easily producible filters to enhance productivity and efficiency, which makes the filter reported here a possible replacement to currently used technology.

Fig. 2b and c show scanning electron microscope images (SEM) of the original filter and the modified filter coated with a cross-linked NFC hydrogel. Compared to the original filter, the SEM image of the modified filter has a coating, which evenly covers the entire filter and reduces its pore size. The differences between the images in Fig. 2b and c clearly show the hydrogel has attached to the surface of the fiber. Fig. 2d and inset image show optical microscope images of the filter in the working state. The image displays the reduced pore size compared to the dry modified filter, as well as the microscopic roughness created by hydrogel on the fibers. By measuring a large number of pores through the optical microscope and calculating the pore size using Hagen–Poiseuille law, the average pore diameter was determined as 23 μm . The microscopic roughness of the hydrogel enhances the oleophobic nature of the hydrated filter. The microscopic pockets created by the roughness trap water, which repels the oil due to its higher surface energy.

Fig. 3a and b show the experimental set up used to examine the flow rate of water through the filter. The hexane was dyed red with oil red-o dye (Sigma Aldrich) and the water kept clear, so the presence of each could be determined visually in the filtered liquid. The hexane-in-water (50 : 50 v : v) emulsion was created using 2.5 mg of sodium dodecyl sulfate (SDS) to 1 mL of water as an emulsifier.⁵ After two hours of mixing at 700 rpm, the water and hexane were clearly mixed when poured into the experimental apparatus, as seen by the consistent pink colour of the emulsion in Fig. 3a. The oil droplets morphology was characterized by microscope, giving an average droplets size of 24 μm . Fig. S2 (ESI[†]) shows a typical microscope image of the emulsion.

The filter was saturated with water and placed at the bottom of a glass graduated cylinder funnel suspended over a beaker placed on a scale (details shown in ESI[†]). The emulsion was poured into the glass graduated cylinder filtration funnel. During filtration, the emulsion stayed above the filter and clear water filtered into the beaker below as shown in Fig. 3b.

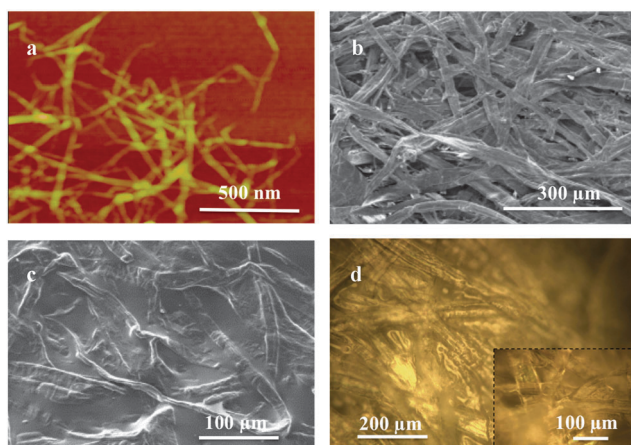


Fig. 2 (a) AFM image of NFC. SEM images of (b) the original filter paper and (c) the hydrogel coated filter crosslinked with citric acid. (d) Optical microscope image of hydrated filter with high roughness. Inset is the high-resolution image of the hydrating filter showing the pores still reserved after NFC hydrogel coating.

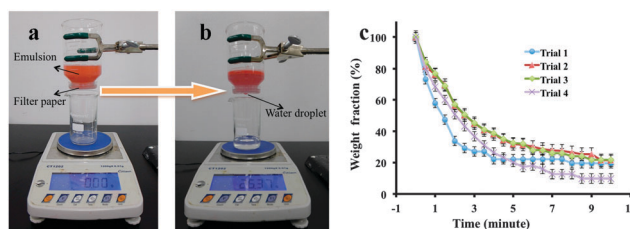


Fig. 3 Images of (a) the set up at the moment filtration starts with the hexane-in-water emulsion above the filter and (b) the set up during filtration as the water passes through the filter and hexane-rich retentate is retained above the filter. (c) A plot of the weight fraction of water retained in the emulsion over time.

The flow rate was determined by measuring the time the amount of liquid took to pass through the filter. The filtered amount was determined by the weight displayed on the scale and the known density of the water (1 mL g^{-1}).

By measuring the weight percentage of water retained in the emulsion *vs.* time shown in the plot in Fig. 3c, the flow rate was determined by the slope of the linear section. The data displays a flux of $89.6 \text{ L m}^{-2} \text{ h}^{-1}$, which is compatible to that of hydro-responsive membranes to separate water rich permeate.¹³ After a certain time, the weight fraction of water retained plateaus at around 20%. This is a result of the experimental set up and gravity driven conditions of the experiment. After an average of 80% weight fraction of water is filtered, there is no longer enough pressure to maintain water filtration. If a continuous flow apparatus was used, adding the emulsion while removing the filtered oil, the weight fraction of water retained *vs.* time plot would have a purely linear behaviour and constant flow rate. After one filtration the flow rate of filter decreases due to some oil coating left over from the previous trial. However, the flow rate becomes constant after the first filtration, showing that no further oil clogging or oil fouling effects the filter. After the trials are complete the filter can be rinsed completely of oil, returning to its original color (Fig. S4, ESI†).

The filter's performance is superior to other recent hydrophilic/oleophobic gravity-driven filters.^{13–15} These filters either have a lower efficiency^{18,25} than the filter in this study or contain fluoride groups.¹⁵ In Kota's study,¹³ although the stainless steel mesh coated with fluorodecyl polyhedral oligomeric silsesquioxane + cross-linked poly(ethylene glycol) diacrylate blend has a similar flow rate of $90 \text{ L m}^{-2} \text{ h}^{-1}$, it takes a full 5 to 10 minutes before the filtration begins due to the need for surface reconfiguration. The filter in this study undergoes immediate filtration, which is advantageous because it decreases the time it takes to filter an emulsion. Other filters with significantly higher flux rates use nanoparticles, nanomaterials, or CNTs,^{11,22,23} which are expensive, make the process difficult to scale, and have possible harmful effects if broken from the filter. Therefore, the filter in this study provides an environmentally safer option, which is also more economically feasible in large-scale production than its recent counterparts because of its simple processing and inexpensive raw materials. These characteristics make this NFC modified filter more advantageous in large scale filter applications, which need an easily replaced, lower cost filter that has a minimal environmental impact such as waste water management, oil refining, or oil spills.

The liquid obtained after filtration was clear, indicating the absence of hexane (Fig. 4b). UV-visible spectroscopy absorption data, shown in Fig. 4a, was taken to determine the specific amount of hexane present in the filtered water. The plot in Fig. 4a shows the filtered water absorption curve closely aligns with the absorption curve for the reference water, while displaying a completely different behaviour than oil red dyed hexane. The oil red dyed hexane samples have typical peaks of absorption at around 348 nm and 512 nm, which is not obviously seen in the filtered sample. These absorption spectra prove that the filtered sample contains water nearly without hexane and that the

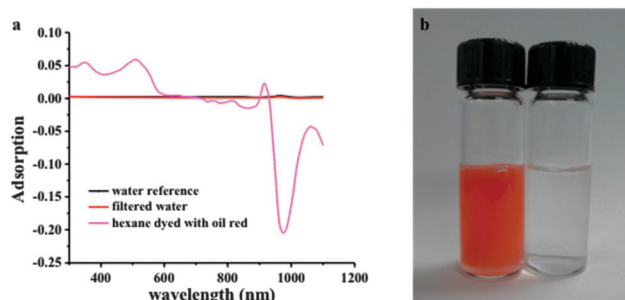


Fig. 4 (a) UV-visible spectroscopy absorption data for water reference, filtered water, and hexane dyed with oil-red. (b) Image of oil red dyed hexane and water emulsion on the left and filtered water on the right.

filter has hydrophilic/oleophobic filtration behaviour. Using the absorption data from Fig. 4a, Beer's law,²⁶ and the standard eqn (1) for determining filtration efficiency,

$$\eta = \left(1 - \frac{C_r}{C_0}\right) \times 100\% \quad (1)$$

where C_r is the concentration of hexane in the filtered water and C_0 is the initial concentration of hexane in the emulsion. The filter's efficiency was calculated at 99.1%.

In conclusion, a novel hydrated oil water separation filters was successfully fabricated with economically and environmentally sound materials and processes, which could easily be scaled up and applied to broad-band filtration applications. The uniqueness of this filter lies in its hydrophilic/oleophobic behaviour derived from the use of cellulose properties at the macroscopic and nanoscopic scale to manipulate surface chemistry instead of the traditionally used toxic chemicals. These properties increase the filter lifetime by decreasing fouling and clogging, as well as making the filter environmentally friendly. The characterization studies proved that the NFC based hydrogel coated the filter fibers creating the hydrophilic/oleophobic nature. Filtration studies displayed a high efficiency of over 99% and a flux of $89.6 \text{ L m}^{-2} \text{ h}^{-1}$ with respect to oil/water emulsion separations, making it a promising high-efficiency filter with positive economic and environmental impacts on oil/water separation applications.

L. Hu acknowledges the startup support from the University of Maryland, College Park and the support from the DOD (Air Force of Scientific Research) Young Investigator Program (FA95501310143). Y. Li would like to thank the Graduate Student Innovation Program of Jiangsu Province (CXLX12_0531) for support. We would like to thank Dr Bonenberger for facility support in taking optical images.

Notes and references

- 1 T. T. Lim and X. Huang, *Ind. Crops Prod.*, 2007, **26**, 125–134.
- 2 Q. Wen, J. Di, L. Jiang, J. Yu and R. Xu, *Chem. Sci.*, 2013, **4**, 591–595.
- 3 L. A. Kovaleva, R. Z. Minnigalimov and R. R. Zinnatullin, *Langmuir*, 2010, **26**, 3050–3057.
- 4 C. S. Fang, B. K. L. Chang, P. M. C. Lai and W. J. Klaila, *Chem. Eng. Commun.*, 1988, **73**, 227–239.
- 5 G. W. Sams and M. Zaouk, *Energy Fuels*, 2000, **14**, 31–37.
- 6 Z. Q. Zhang, G. Y. Xu, F. Wang, S. L. Dong and Y. J. Chen, *J. Colloid Interface Sci.*, 2005, **282**, 1–4.

- 7 Y. Shang, Y. Shi, A. Raza, L. Yang, X. Mao, B. Ding and J. Yu, *Nanoscale*, 2012, **4**, 7874.
- 8 L. Feng, Z. Zhang, Z. Mai, Y. Ma, B. Liu, L. Jiang and D. Zhu, *Angew. Chem., Int. Ed.*, 2004, **116**, 2046–2048.
- 9 X. Huang and T. T. Lim, *Desalination*, 2006, **190**, 295–307.
- 10 S. Maphutha, K. Moothi, M. Meyyappan and S. E. Lyuke, *Sci. Rep.*, 2013, **3**, 1509.
- 11 Z. Xue, S. Wang, L. Lin, L. Chen, M. Liu, L. Feng and L. Jiang, *Adv. Mater.*, 2011, **23**, 4270–4273.
- 12 R. C. B. Lemons, E. B. de Silva, A. dos Santos, R. C. L. Guimaraes, B. M. S. Ferreira, R. A. Guarnieri, C. Dariva, E. Franceschi, A. F. Santos and M. Fortung, *Energy Fuels*, 2010, **24**, 4439–4444.
- 13 A. K. Kota, G. Kwon, W. Choi, J. M. Mabry and A. Tutenja, *Nat. Commun.*, 2012, **3**, 1025.
- 14 X. Zhu, H. Loo and R. Bai, *J. Membr. Sci.*, 2013, **436**, 47–56.
- 15 J. A. Howarter and J. P. Youngblood, *J. Colloid Interface Sci.*, 2009, **329**, 127–132.
- 16 N. M. Kocherginsky, C. L. Tan and W. F. Lu, *J. Membr. Sci.*, 2003, **220**, 117–128.
- 17 J. Zeng and Z. Guo, *Colloids Surf., A*, 2014, **444**, 283–288.
- 18 Y. Wang, S. Tao and Y. An, *J. Mater. Chem. A*, 2013, **1**, 1701–1708.
- 19 Y. Li, H. Zhu, H. Gu, H. Dai, Z. Fang, N. Weadock, Z. Guo and L. Hu, *J. Mater. Chem. A*, 2013, **1**, 15278–15283.
- 20 C. Demitri, R. D. Sole, F. Scalera, A. Sannino, G. Vasapollo, A. Maffezzoli, L. Ambrosio and L. Nicolais, *J. Appl. Polym. Sci.*, 2008, **110**, 2453–2460.
- 21 H. Karimnezhad, L. Rajabi, E. Salehi, A. A. Derakhshan and S. Azimi, *Appl. Surf. Sci.*, 2014, **293**, 275–286.
- 22 J. Lee, C. Y. Tang and F. Huo, *Sci. Rep.*, 2014, **4**, 3740.
- 23 H. Li, Y. Cao, J. Qing, X. Jie, T. Wang, J. Liu and Q. Yuan, *J. Membr. Sci.*, 2006, **279**, 328–335.
- 24 L. Li, L. Ding, Z. Tu, Y. Wan, D. Causse and J. Lanoiselle, *J. Membr. Sci.*, 2009, **342**, 70–79.
- 25 Y. Wang, S. Tao and Y. An, *J. Mater. Chem. A*, 2013, **1**, 1701–1708.
- 26 H. L. Friedman, *J. Chem. Phys.*, 1953, **21**, 319.